**Thermodynamics Project Report**

Mechanical Engineering 3501

Dr. Jung Hyun Kim

GTA Sunday Agbo

Isaac Einstein, Amanda Weiskind, and Avery Zwayer

April 25, 2023

## Table of Contents

## Problem 1

Below is the plant diagram of ORC power plant.

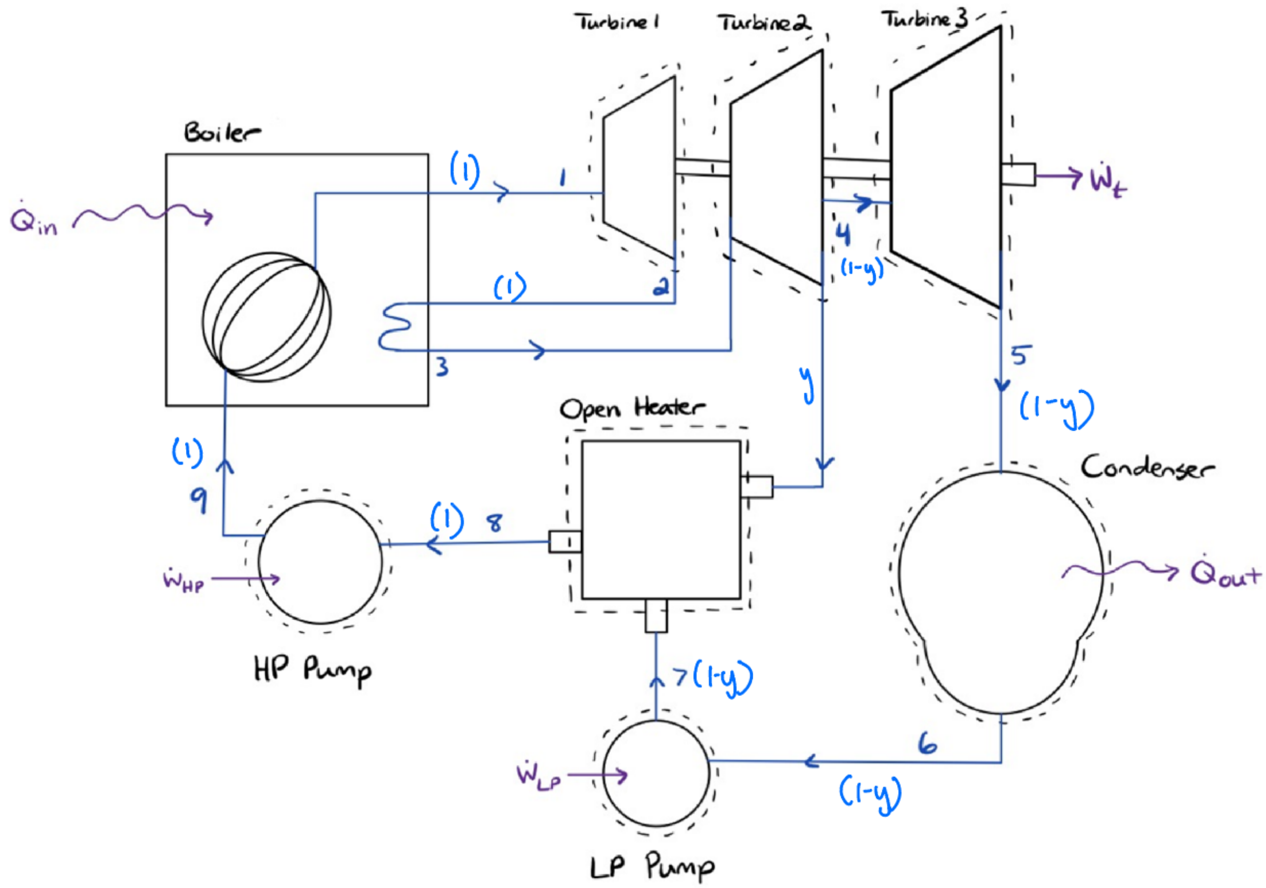


Figure 1: ORC Power Plant Diagram

## Problem 2

Below is the T-s Diagram of the ORC power plant.

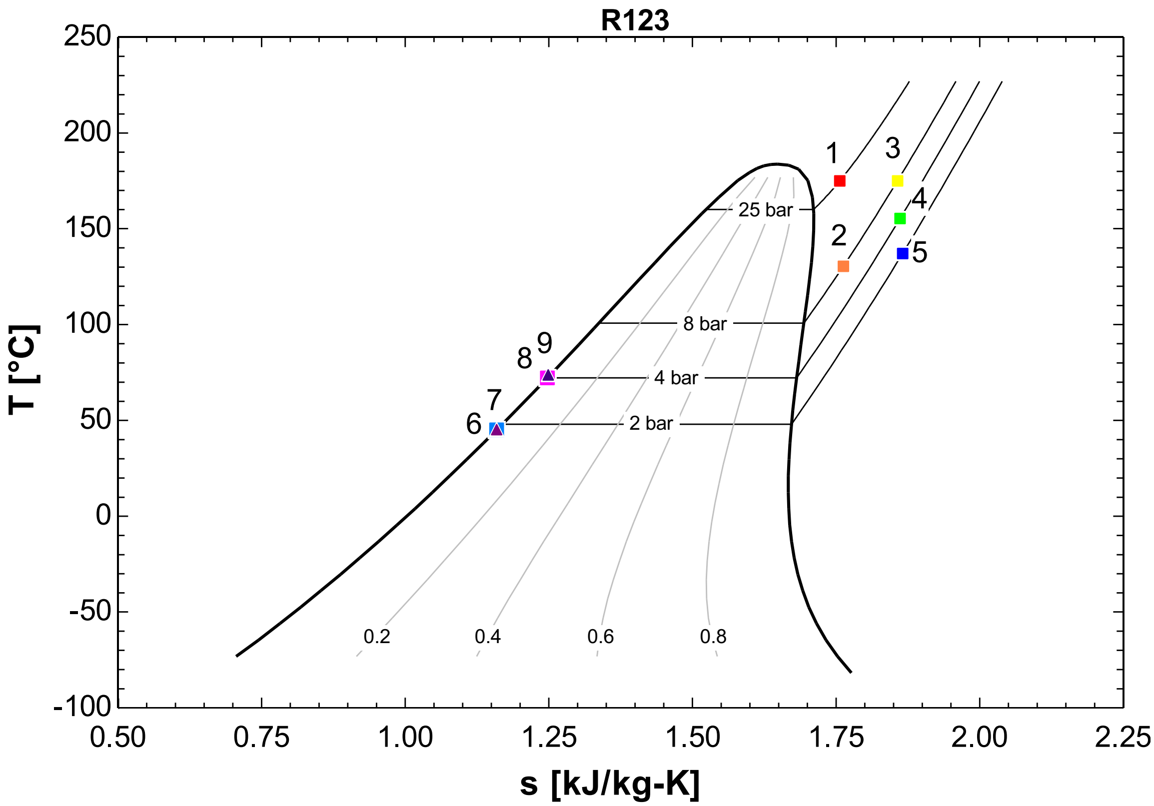


Figure 2: T-s Diagram of ORC

## Problem 3

Below is EES solution window of the ORC with nominal values.

**Unit Settings: SI C bar kJ mass deg**

| | | | | |
|---|---|---|---|---|
| $\boxed{bwr = 0.05139}$ | $\boxed{\eta = 0.1674}$ | $\eta_p$ = 0.75 | $\eta_t$ = 0.88 | h1 = 488.2 [kJ/kg] |
| h2 = 469.8 [kJ/kg] | h2s = 467.2 [kJ/kg] | h3 = 510.3 [kJ/kg] | h4 = 496.6 [kJ/kg] | h4s = 494.7 [kJ/kg] |
| h5 = 483.1 [kJ/kg] | h5s = 481.2 [kJ/kg] | h6 = 247.2 [kJ/kg] | h7 = 247.4 [kJ/kg] | h7s = 247.4 [kJ/kg] |
| h8 = 276.8 [kJ/kg] | h9 = 278.9 [kJ/kg] | h9s = 278.4 [kJ/kg] | p1 = 25 [bar] | p2 = 8 [bar] |
| p2s = 8 [bar] | p3 = 8 [bar] | p4 = 4 [bar] | p4s = 4 [bar] | p5 = 2 [bar] |
| p5s = 2 [bar] | p6 = 2 [bar] | p7 = 4 [bar] | p7s = 4 [bar] | p8 = 4 [bar] |
| p9 = 25 [bar] | p9s = 25 [bar] | $\boxed{Q_{in} = 249.9 \text{ [kJ/kg]}}$ | $\boxed{Q_{out} = 208 \text{ [kJ/kg]}}$ | s1 = 1.756 [kJ/kg-K] |
| s2 = 1.763 [kJ/kg-K] | s2s = 1.756 [kJ/kg-K] | s3 = 1.857 [kJ/kg-K] | s4 = 1.861 [kJ/kg-K] | s4s = 1.857 [kJ/kg-K] |
| s5 = 1.866 [kJ/kg-K] | s5s = 1.861 [kJ/kg-K] | s6 = 1.159 [kJ/kg-K] | s7 = 1.159 [kJ/kg-K] | s7s = 1.159 [kJ/kg-K] |
| s8 = 1.248 [kJ/kg-K] | s9 = 1.249 [kJ/kg-K] | s9s = 1.248 [kJ/kg-K] | T1 = 175 [C] | T2 = 130.4 [C] |
| T2s = 127.6 [C] | T3 = 175 [C] | T4 = 155.3 [C] | T4s = 153.1 [C] | T5 = 137.1 [C] |
| T5s = 134.9 [C] | T6 = 45 [C] | T7 = 45.13 [C] | T7s = 45.08 [C] | T8 = 72.15 [C] |
| T9 = 73.71 [C] | T9s = 73.23 [C] | $W_{in}$ = 2.266 [kJ/kg] | $W_{net}$ = 41.83 [kJ/kg] | $W_{out}$ = 44.1 [kJ/kg] |
| $W_{p1}$ = 0.167 [kJ/kg] | $W_{p2}$ = 2.099 [kJ/kg] | $W_{t1}$ = 18.44 [kJ/kg] | $W_{t2}$ = 13.74 [kJ/kg] | $W_{t3}$ = 11.92 [kJ/kg] |
| x8 = 0 | $\boxed{y = 0.1179}$ | | | |

Figure 3: EES Solution Window with Nominal Values.

## Problem 4

### Problem 4-A

Below is the EES solution window of the ORC when optimizing the pressure at state 2.

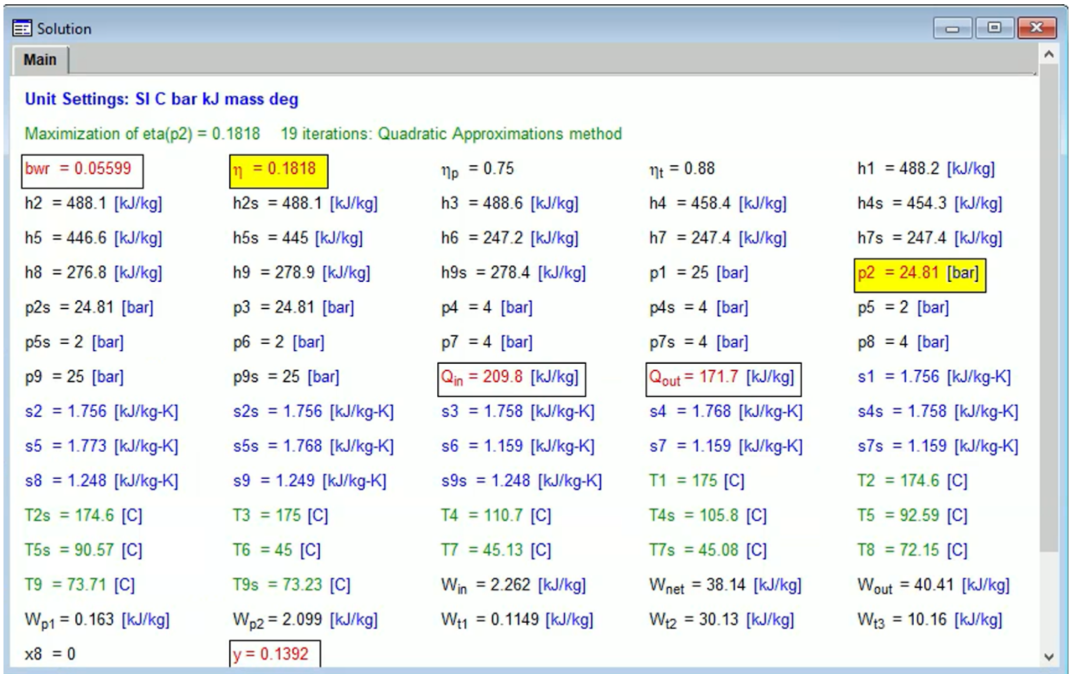


Figure 4: EES Solution Window Optimizing p2.

With the optimized pressure at state two of 24.81 bar compared to 8 bar nominally, the thermal efficiency increases from 0.1674 to 0.1818 by optimization. Additionally, when optimizing the pressure at state two, the work from turbine one decreases to approximately zero and the work from turbine two increases substantially. The overall work output, Wnet, increases when optimizing the pressure at state two, even with the decreased output from turbine one. Therefore, the cycle could be simplified by removing turbine one and raising the pressure at state two entering turbine two.

The code was adjusted to confirm this. Turbine one was taken out as well as the reheat cycle which would now be unnecessary. Without turbine one, the work output was essentially the same at 40 [kJ/kg], and the efficiency of the system was still 0.182. Thus, our adjusted code confirms that removing turbine one and raising the pressure entering turbine two to 24.81 [bar] simplifies the cycle without changing any of the output variables.

Below is a depiction of the difference between the original cycle and our described simplified cycle. Additionally, the solution window for code that removed turbine 1 and the reheat section is included.

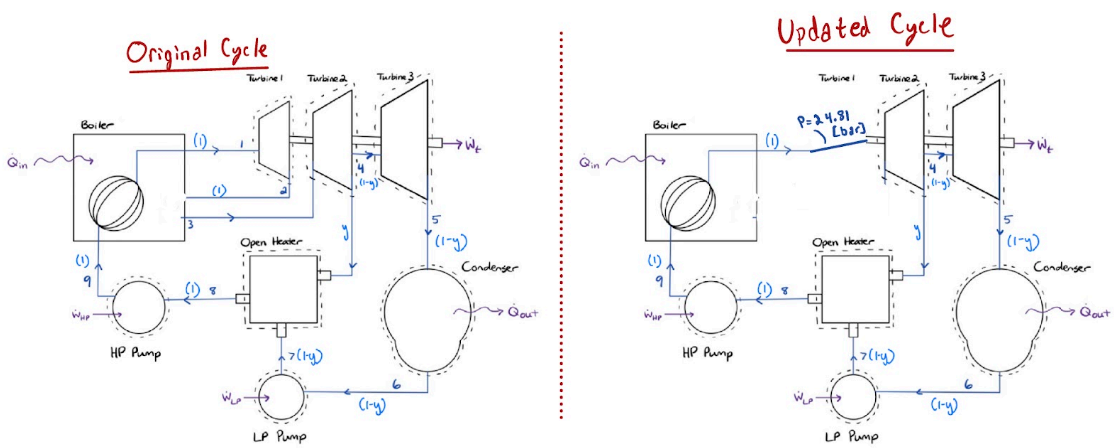


Figure 5: Original Cycle vs. Simplified Cycle

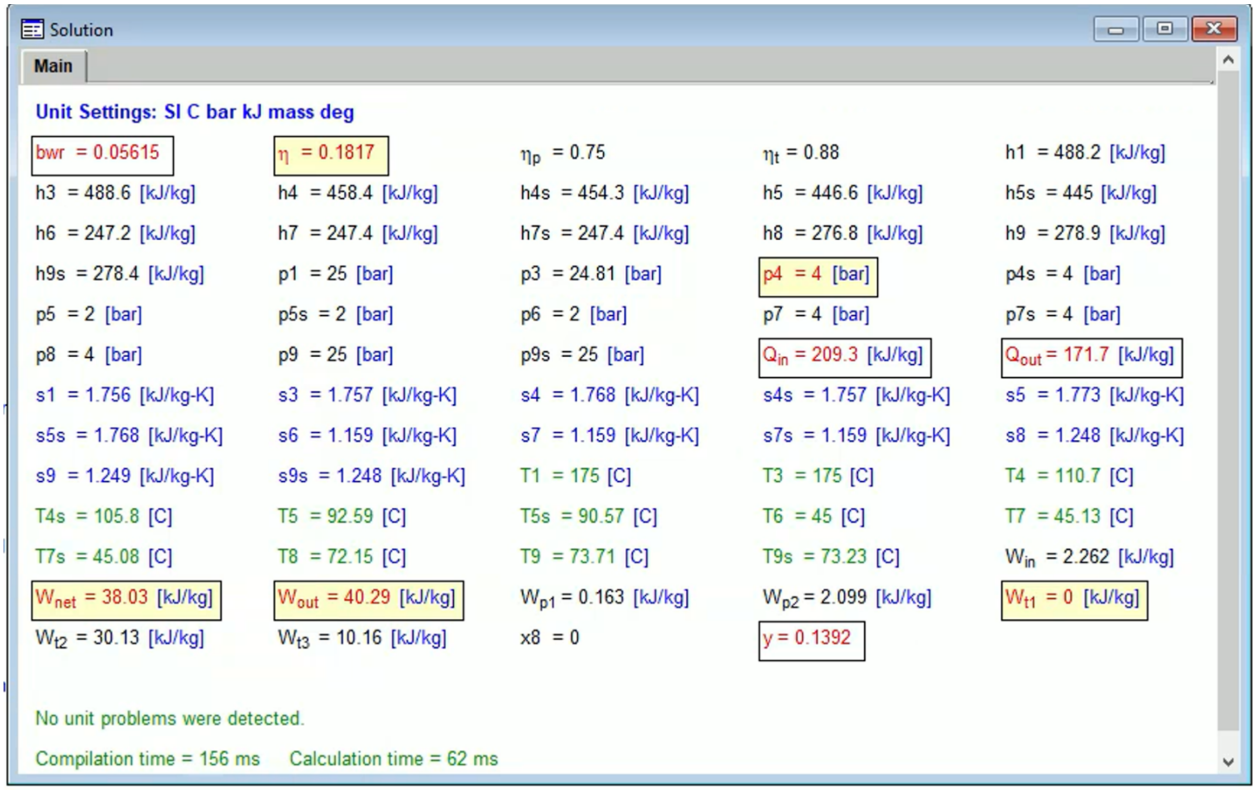


Figure 6: Original Cycle vs. Simplified Cycle

## Problem 4-B

Below is the EES solution window of the ORC when optimizing pressure at state 4.

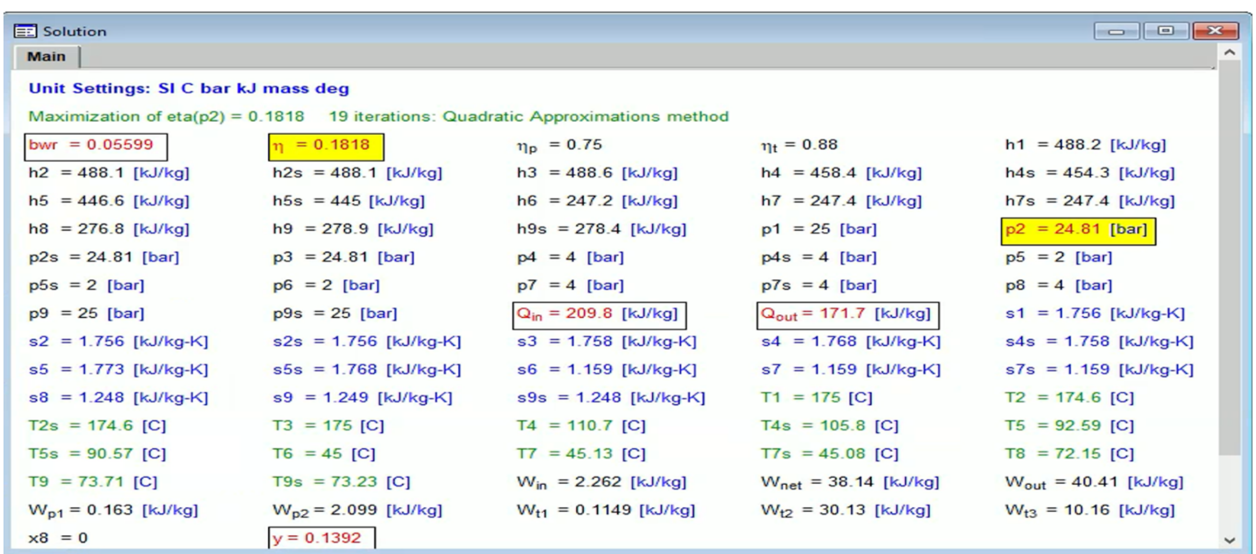


Figure 7: Solution Window Optimizing p4

With the optimized pressure at state four of 6.887 bar compared to 4 bar nominally, the thermal efficiency increases from 0.1674 to 0.1703 with the optimized pressure.

## Problem 4-C

Below is the EES solution window for part 4-C when optimizing pressure at state four with the previously optimized value of p2 from part 4-A replacing the nominal value.

**Unit Settings: SI C bar kJ mass deg**

Maximization of eta(p4) = 0.1878 18 iterations: Quadratic Approximations method

| | | | | | |
|---|---|---|---|---|---|
| bwr = 0.06354 | $\eta$ = 0.1878 | $\eta_p$ = 0.75 | $\eta_t$ = 0.88 | h1 = 488.2 [kJ/kg] | h2 = 488.1 [kJ/kg] |
| h2s = 488.1 [kJ/kg] | h3 = 488.6 [kJ/kg] | h4 = 471.1 [kJ/kg] | h4s = 468.7 [kJ/kg] | h5 = 446.6 [kJ/kg] | h5s = 443.2 [kJ/kg] |
| h6 = 247.2 [kJ/kg] | h7 = 247.8 [kJ/kg] | h7s = 247.7 [kJ/kg] | h8 = 312.4 [kJ/kg] | h9 = 314.2 [kJ/kg] | h9s = 313.8 [kJ/kg] |
| p1 = 25 [bar] | p2 = 24.81 [bar] | p2s = 24.81 [bar] | p3 = 24.81 [bar] | p4 = 8.447 [bar] | p4s = 8.447 [bar] |
| p5 = 2 [bar] | p5s = 2 [bar] | p6 = 2 [bar] | p7 = 8.447 [bar] | p7s = 8.447 [bar] | p8 = 8.447 [bar] |
| p9 = 25 [bar] | p9s = 25 [bar] | $Q_{in}$ = 174.5 [kJ/kg] | $Q_{out}$ = 141.7 [kJ/kg] | s1 = 1.756 [kJ/kg-K] | s2 = 1.756 [kJ/kg-K |
| s2s = 1.756 [kJ/kg-K] | s3 = 1.757 [kJ/kg-K] | s4 = 1.763 [kJ/kg-K] | s4s = 1.757 [kJ/kg-K] | s5 = 1.772 [kJ/kg-K] | s5s = 1.763 [kJ/kg-I |
| s6 = 1.159 [kJ/kg-K] | s7 = 1.16 [kJ/kg-K] | s7s = 1.159 [kJ/kg-K] | s8 = 1.345 [kJ/kg-K] | s9 = 1.346 [kJ/kg-K] | s9s = 1.345 [kJ/kg-I |
| T1 = 175 [C] | T2 = 174.6 [C] | T2s = 174.6 [C] | T3 = 175 [C] | T4 = 132.6 [C] | T4s = 130 [C] |
| T5 = 92.54 [C] | T5s = 88.33 [C] | T6 = 45 [C] | T7 = 45.41 [C] | T7s = 45.26 [C] | T8 = 103.2 [C] |
| T9 = 104.8 [C] | T9s = 104.4 [C] | $W_{in}$ = 2.224 [kJ/kg] | $W_{net}$ = 32.77 [kJ/kg] | $W_{out}$ = 34.99 [kJ/kg] | $W_{p1}$ = 0.4336 [kJ/kg |
| $W_{p2}$ = 1.79 [kJ/kg] | $W_{t1}$ = 0.1138 [kJ/kg] | $W_{t2}$ = 17.45 [kJ/kg] | $W_{t3}$ = 17.43 [kJ/kg] | x8 = 0 | y = 0.2893 |

Figure 8: EES Solution Window Optimizing p4 with Previously Optimized Value of p2

Using the optimal value of p2, an optimum value of p4=8.447 bar correlates with the optimum efficiency of 0.1878. The optimum efficiency for this part is slightly improved from the previous parts 4-A and 4-B.

## Problem 4-D

Below is the EES solution window for part 4-D when optimizing pressures at states two and four.

Figure 8: EES Solution Window Optimizing p2 and p4.

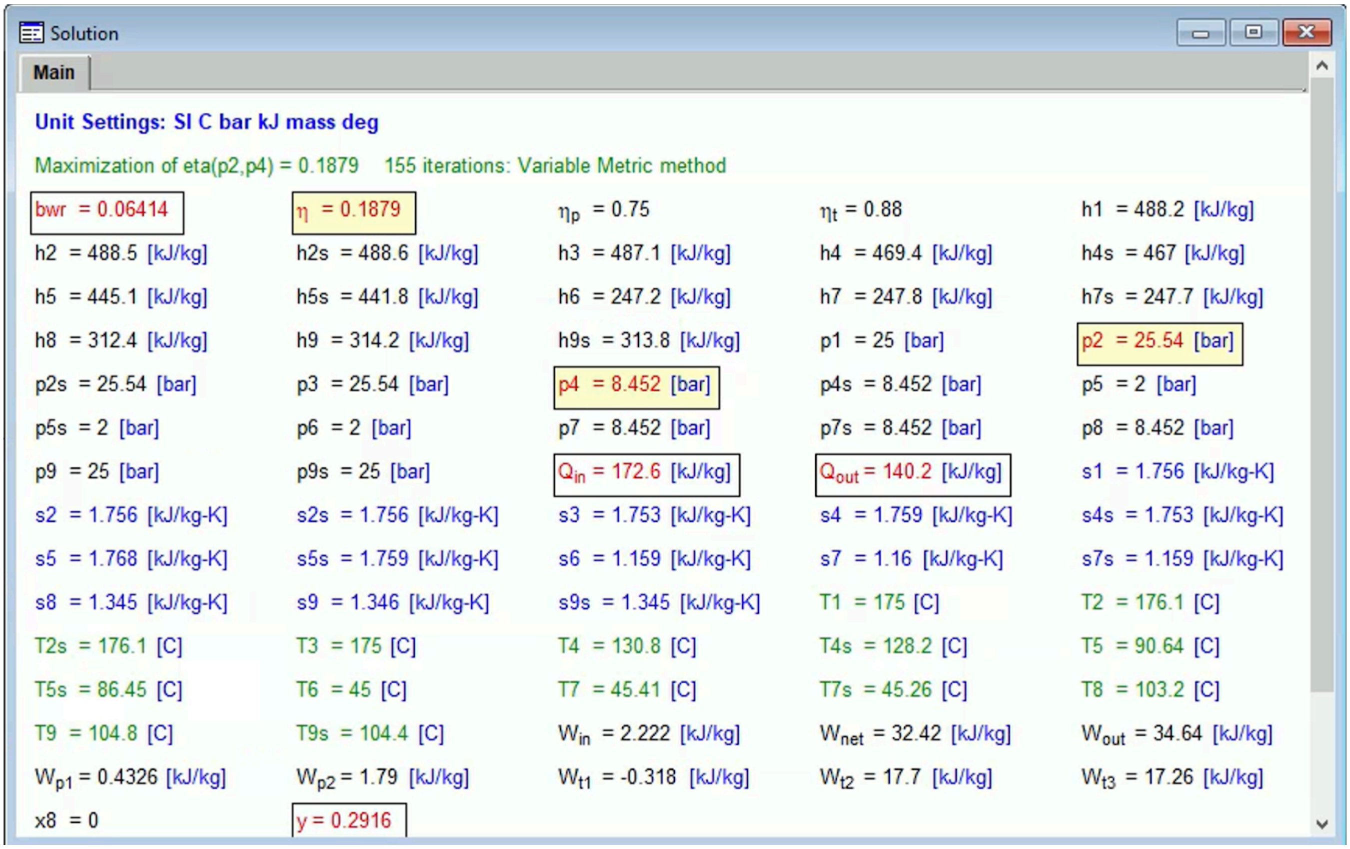


Figure 9: EES Solution Window Optimizing p2 and p4

Correlating with the optimal efficiency of 0.1879 is an optimum value of p4= 8.45 bar, and p2=25.54 bar. The efficiency in this part is only 0.0001 higher than in part 4-C, further confirming the results.

# Problem 5

## Problem 5-A

In problem 5-A, the optimal pressure values, p2 and p4, from problem 4-D were used while varying the temperature at state one parametrically to determine the limits of operation, as shown in Table 1 below.

Table 1: Parametric variation of T1 effects on efficiency, mass fraction, and quality at state 1.

| $T1$ [C] | $\eta$ | $y$ | $x1$ |
|---|---|---|---|
| 150 | 0.1391 | 0.5429 | -100 |
| 155 | 0.1468 | 0.5148 | -100 |
| 160 | 0.1543 | 0.488 | -100 |
| 165 | 0.188 | 0.3085 | 100 |
| 170 | 0.188 | 0.2995 | 100 |
| 175 | 0.1879 | 0.2916 | 100 |
| 180 | 0.1876 | 0.2844 | 100 |
| 185 | 0.1872 | 0.2777 | 100 |
| 190 | 0.1868 | 0.2715 | 100 |
| 200 | 0.1858 | 0.2602 | 100 |

As shown in Figure 6, the thermal efficiency is maximized for state one temperature values above 165ºC.

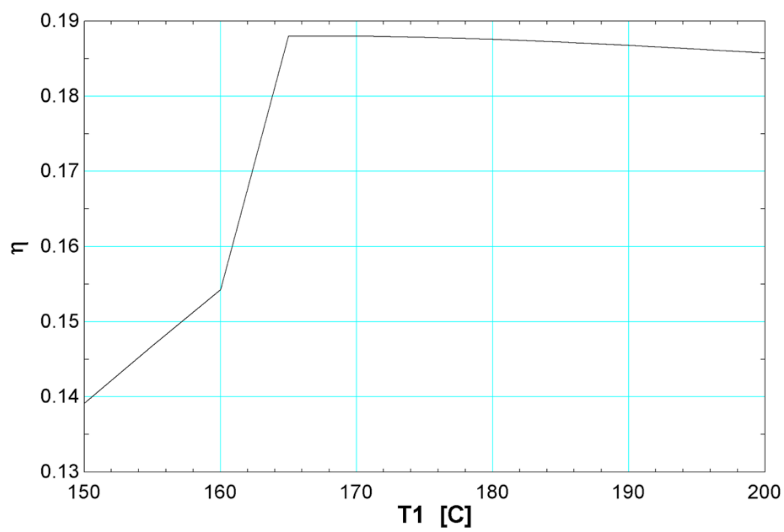


Figure 10: Plot of T1 vs. Thermal Efficiency.

As shown in Figure 7, the working fluid is within the vapor dome from 160°C to 165°C. Given that turbines operate with a saturated vapor working fluid input (quality x1=100), temperature values above 165ºC are within the limits of operation.

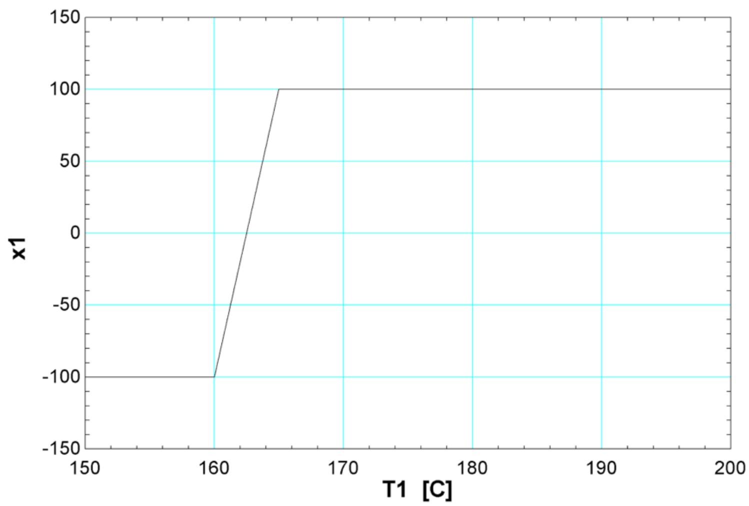


Figure 11: Plot of T1 vs. Quality at State 1, x1.

Finally, the mass fraction, y, should be a positive value to be a physically valid solution which is verified for the same temperature range in Figure 8. Therefore, the limits of operation for temperature values at state one, from the 150 to 200°C range tested, contains values greater than or equal to 165°C.

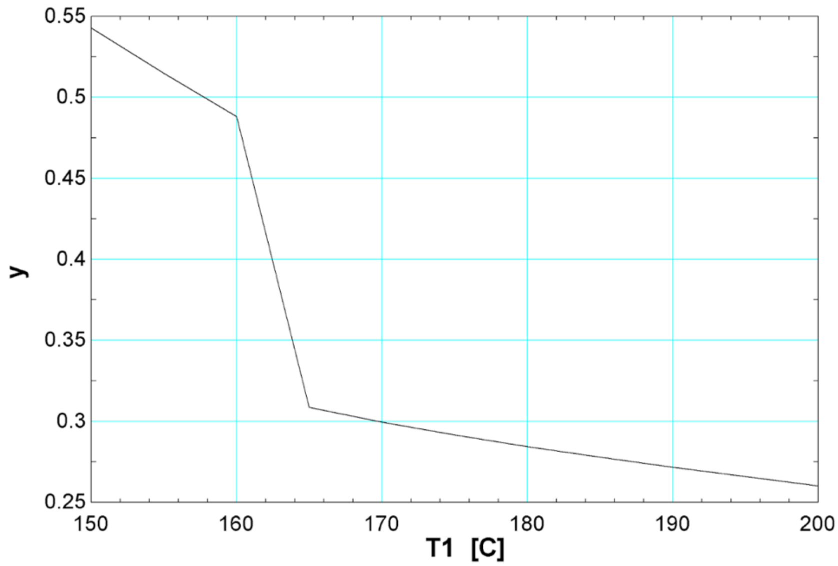


Figure 12: Plot of T1 vs. Mass Fraction, y.

## Problem 5-B

In problem 5-B, the optimal pressure values, p2 and p4, from problem 4-D were used while varying the temperature at state six parametrically to determine the limits of operation, as shown in Table 2 below.

Table 2: Parametric variation of T6 effects on efficiency, mass fraction, and quality at state 6.

| $T6\ [C]$ | $\eta$ | $x6$ | $y$ |
|---|---|---|---|
| 20 | 0.1777 | -100 | 0.3664 |
| 21 | 0.178 | -100 | 0.3638 |
| 22 | 0.1784 | -100 | 0.3611 |
| 23 | 0.1787 | -100 | 0.3584 |
| 24 | 0.1791 | -100 | 0.3557 |
| 25 | 0.1795 | -100 | 0.353 |
| 26 | 0.1799 | -100 | 0.3502 |
| 27 | 0.1803 | -100 | 0.3474 |
| 28 | 0.1806 | -100 | 0.3445 |
| 29 | 0.181 | -100 | 0.3417 |
| 30 | 0.1814 | -100 | 0.3388 |
| 31 | 0.1818 | -100 | 0.3359 |
| 32 | 0.1822 | -100 | 0.3329 |
| 33 | 0.1826 | -100 | 0.3299 |
| 34 | 0.183 | -100 | 0.3269 |
| 35 | 0.1835 | -100 | 0.3239 |

| | | | |
|---|---|---|---|
| 36 | 0.1839 | -100 | 0.3208 |
| 37 | 0.1843 | -100 | 0.3177 |
| 38 | 0.1847 | -100 | 0.3146 |
| 39 | 0.1852 | -100 | 0.3114 |
| 40 | 0.1856 | -100 | 0.3082 |
| 41 | 0.186 | -100 | 0.3049 |
| 42 | 0.1865 | -100 | 0.3016 |
| 43 | 0.1869 | -100 | 0.2983 |
| 44 | 0.1874 | -100 | 0.295 |
| 45 | 0.1879 | -100 | 0.2916 |
| 46 | 0.1883 | -100 | 0.2882 |
| 47 | 0.1888 | -100 | 0.2847 |
| 48 | 0.1893 | -100 | 0.2812 |
| 50 | -0.1938 | 100 | -5.534 |

The optimal limits of operation for temperature values at state six range from 20ºC to 48ºC. On the thermal efficiency versus T6 plot in Figure _, the system's efficiency decreases with temperatures above T6=48, which is not desirable.

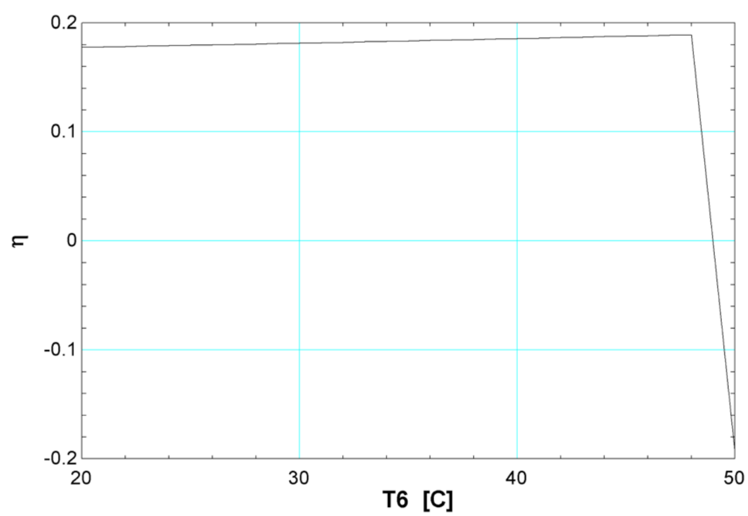


Figure 13: Plot of T6 vs. Thermal Efficiency.

These non-desirable efficiencies at the higher temperatures are verified on the mass fraction versus T6 plot in Figure __ where the mass fraction becomes negative with temperatures greater than T6=48ºC, which is not physically valid.

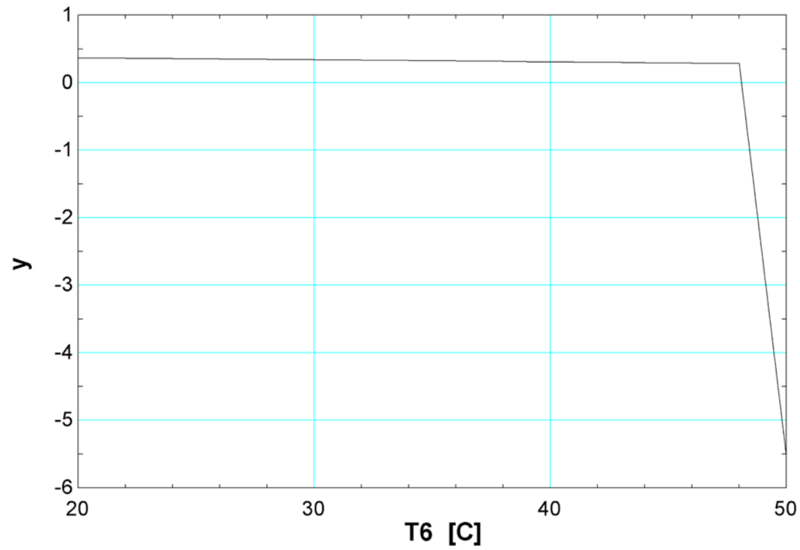


Figure 13: Plot of T6 vs. Mass Fraction, y.

Further, this is verified on the x6 versus T6 plot in Figure __ shown below as the quality should indicate a saturated liquid exiting the condenser (x6 = -100) which is true for lower temperatures.

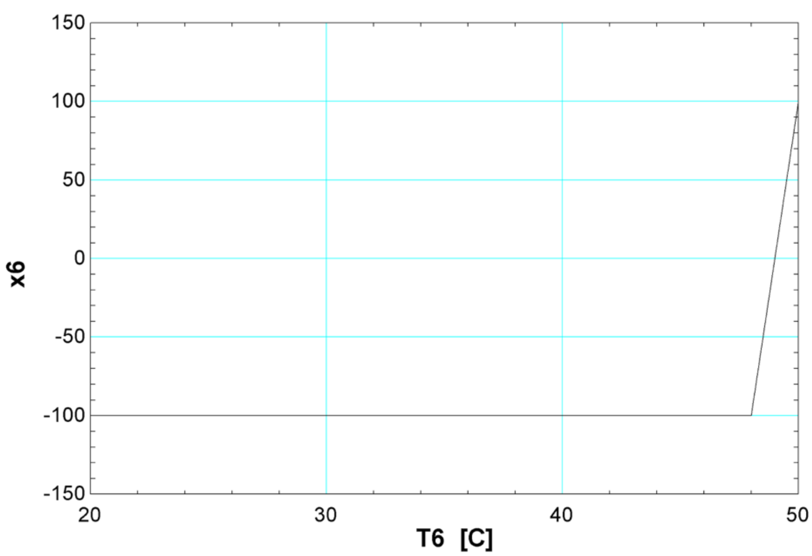


Figure 14: Plot of T6 vs. Quality at State 6, x6.

## Conclusion

The cycle investigated in this report is an Organic Rankine Cycle (ORC) powered by the sun. Different parameters were optimized while monitoring the resultant efficiency of the cycle.

In part four, the pressure of the state entering turbine 2 and the state entering turbine 4 were analyzed and optimized. It was found that optimizing pressures 2 and 4 together produced an increased thermal efficiency compared to optimizing pressure 4 alone. However, optimizing pressure 2 led to the same cycle efficiency as optimizing pressures 2 and 4 together. Based on the calculated results in part 4-A (optimizing pressure 2 alone), the cycle can likely be simplified by removing turbine 1 and optimizing the pressure of the state going into turbine 2. With the optimized pressure entering turbine 2, the work and efficiency provided by turbine 1 and the ensuing reheating section were negligible.

In part five, the temperatures entering turbine 1 and (state 1) and leaving the condenser (state 6) were varied parametrically. T-S graphs of these parametric tables were used to determine the optimal cycle efficiency. The quality for state 1 had to be greater than or equal to 100 meaning the state was a saturated vapor; the quality for state 6 had to be less than or equal to -100 meaning the state was condensed liquid. The maximum thermal efficiency within valid quality ranges were graphically determined illustrating the optimal conditions for this cycle.